

# Experimenting and Simulating Thermoelectric Cooling of an LED Module

<http://dx.doi.org/10.3991/ijoe.v11i4.4692>

Mika Maaspuro  
Aalto University, Aalto, Finland

**Abstract** — Use of a thermoelectric component (TEC) for an LED module cooling will be studied. The issue will be approached by revealing the operation of a thermoelectric component known also as Peltier element, and the main equations describing its behaviour. An experimental setup including an LED module, a TEC, an heatsink and a fan will be build. Heat dissipation and the electrical performance measurements of the hole experimental setup will be conducted. The benefits and the limitations of TEC used in cooling, will be revealed. Cooling effect versus used electrical power will be studied. 3D thermal simulations for the experimental setup using a FEM simulation software will be presented. Alternatively, a standard circuit simulator will be used. A spice model, which imports TEC's parameters from the data sheet, will be developed. The spice simulation results are compared with the experimental results.

**Index Terms** — FEM-simulations, LED thermal management, thermoelectric cooling.

## I. INTRODUCTION

Thermal management is important for maintaining a stable light production and lifetime of an LED. Reduction in the LED junction temperature increases the light production and extends the lifetime. Proper thermal management requires the use of heat dissipation device. These can be either passive or active devices. The active heat dissipation devices, practically cooling devices, are fans, microchannel coolers, heat exchangers and thermoelectric components (TEC). Usually active heat dissipation requires the use of some passive cooling devices, most often heatsinks. A heat pipe is a very efficient cooling device. Using a heat pipe with TEC has been studied by [1]. A heatsink (HS) as a single cooling device is widely used as well. Heatsink with a fan (HSF) is a widely used cooling arrangement. This study focus on the cooling arrangements which use either HS, HSF or TEC with HSF.

TEC has some good characteristics. The cooling effect is fast. Without moving parts, TEC provides silent and maintenance-free operation. TEC can cool LED even below the ambient temperature. This is not possible by using HS or HSF. TEC is a solid state device of high reliability having MTBF higher than 100 000 hours. Its MTBF is in the same range as LED's. TEC features high stability and it is accurately controlled by the electric current which flows through it. The effective use of TEC requires HS, HSF, or some other heat convection device

mounted on the hot side. TEC is a small size and a relative inexpensive component. Therefore TECs are widely used in many applications.

TEC has some significant drawbacks. It does not fit well in high efficiency devices. Efficiency is related to figure-of-merit  $ZT$ , which for present day TEC is close to 1 [2]. Efficiency is the highest at negligible output power level but reduces at higher levels [3]. TEC generates Joule heating according to its ohmic resistance and the electric current which flows through it. This heat must be removed also by the HS or the HSF mounted on the TEC. Use of TEC as an active cooling device for LEDs has been studied by authors [4-6]. In those studies, TEC is used with passive cooling devices. Compared with passive cooling alone, the addition of TEC makes it possible to reach much lower LED junction temperature. Using TEC as part of a cooling system can be a practical solution in some specific applications of LED lighting. Applications where the lighting device should remain at very low temperature. Applications where extremely stable light levels and fast lighting control are requested. Applications where long operation life and maintenance free operation are requested. The most common application of TEC in LED lighting might be a light source for microscopy use where both the light intensity and the wavelength stability are requested.

## II. THERMOELECTRIC COMPONENT

TEC is able to generate temperature difference  $\Delta T$  between its cold and hot side. While the electric current flows through the component, the cold side gets cooler and the hot side warmer. By reversing the direction of the electric current, reverse the cold and sides as well. Just a few equations are needed to describe the operation of TEC. The equations for the heat flow through the cold  $q_c$  and the hot side  $q_h$  are:

$$q_c = \frac{\Delta T}{\theta_m} + \alpha_m T_c I - \frac{1}{2} I^2 R_m \quad (1)$$

$$q_h = \frac{\Delta T}{\theta_m} + \alpha_m T_h I + \frac{1}{2} I^2 R_m \quad (2)$$

While an electric current  $I$  flows through the component, a voltage  $V$  will be measured over it.

$$V = \alpha_m T_h - \alpha_m T_c = \alpha_m \Delta T \quad (3)$$

Where  $\alpha_m$  is the Seebeck coefficient,  $\theta_m^{-1}$  the thermal resistance of the element and  $R_m$  is the electrical resistance of the element. TEC is made of  $N$  pellets, which are made of suitable semiconductor material, most often bismuth telluride. These pellets are arranged by pairs, each of them has one n-type and one p-type component. All the pellets are connected electrically in series and thermally in parallel. This means the total  $\alpha_m' = N \cdot \alpha_m$ ,  $R_m' = N \cdot R_m$  and  $\theta_m' = \theta_m/N$ . Equations (1-3) are able to explain the basic operation of TEC. Normally, some other equations are presented to better qualify the TEC. The general quality of TEC is the figure-of-merit,  $ZT$  which is defined as

$$ZT = \frac{\alpha_m \theta_m}{R_m} \quad (4)$$

High  $ZT$  is desired. For a high value of  $ZT$ , both the Seebeck coefficient and thermal resistance should be maximized and at the same time  $R_m$  should be minimized. Another measure for the quality of TEC is the coefficient of performance COP. This is defined as

$$COP = \frac{q_c}{\alpha_m I \Delta T + I^2 R_m} \quad (5)$$

It can be seen from Equ. 5 that Joule heating generated by the electrical resistance  $R_m$  is the major reason which reduces COP. COP gives a measure of how much heat can be absorbed on the cool side at certain temperature difference  $\Delta T$  and electric current  $I$ . Material characteristics are temperature dependent [7]. The review study of bismuth telluride [2] shows that maximum  $ZT$  can be even 1.5 for p-type and 1.2 for n-type material, and the maximum is reached at elevated temperatures.

### III. EXPERIMENTAL WORK

For the experimental work, a setup shown in Fig. 1. has been manufactured. It has an LED module mounted on a thick aluminium plate. The LED module is type Xlamp CXA2011 (Cree). The aluminium plates serve as a heat spreaders and they are made wide enough that temperature sensors can easily be mounted on it. The TEC module can be mounted on the aluminium plate. The TEC module is type TEC1-12706 (Hebei I.T Co. Ltd. Shanghai). It has dimensions of 40 mm x 40 mm x 3.9 mm and its  $Q_{max}$  is specified to 57 W. Above the TEC, there is another aluminium plate. A finned heatsink is mounted on the aluminium plate. The heatsink has dimensions of 60 mm x 60 mm x 35 mm. Small amount of thermal interface material (TIM) is used between the surfaces. Standard silicone based cream has been used. Top of the heatsink is a fan. The maximum electrical power of the fan is 2 W. An efficient cooling effect can be

reached at low air speed and therefore the fan is operated at 0.5W. The hole setup stands on bars which are thermally isolated from the setup and from the environment. For temperature measurements, there are fixtures for type K thermo-couples on each aluminium plate and on the heatsink. Resolution in the temperature measurements is  $\pm 1$  °C, but accuracy is better than this.

The setup uses an LED driver, which is controlled by computer software via DALI, Digital Addressable Lighting Interface. The benefit of DALI control in this experiment is that power settings can be done and repeated accurately. The maximum electrical power the driver can source for the LED module is 15.2 W. Measurements have been done at four input electrical power levels.

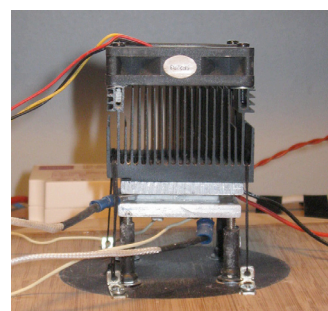


Figure 1. The LED module, the aluminium plates, the TEC, the heatsink, the fan, and the thermocouples. The system is standing on thermally isolated bars.

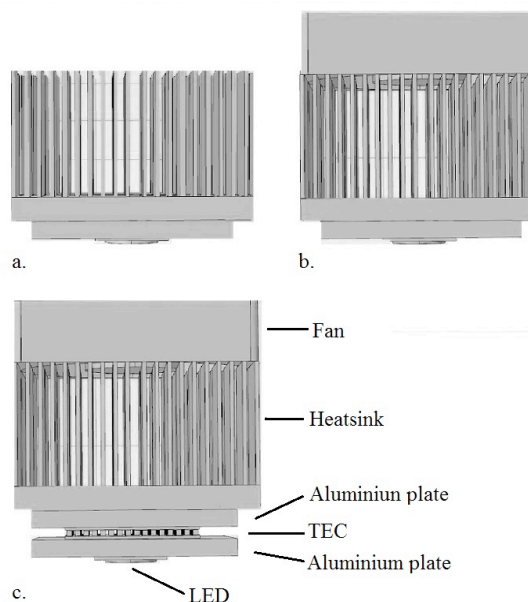


Figure 2. The measured setups. a) LED, aluminium plate and heatsink. b) LED, aluminium plate and fan. c) LED, two aluminium plates, TEC, heatsink and fan. TIM is used between the LED and the plates and between the plates and the TEC and between the plate and the heatsink. The heatsink has size of 60 mm x 60 mm x 35 mm. The aluminium plates have size of 50 mm x 50 mm x 5 mm.

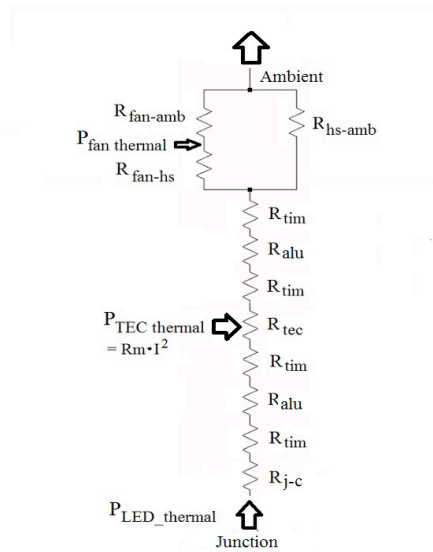


Figure 3. Thermal model for case c. The arrows are indicating heat fluxes.

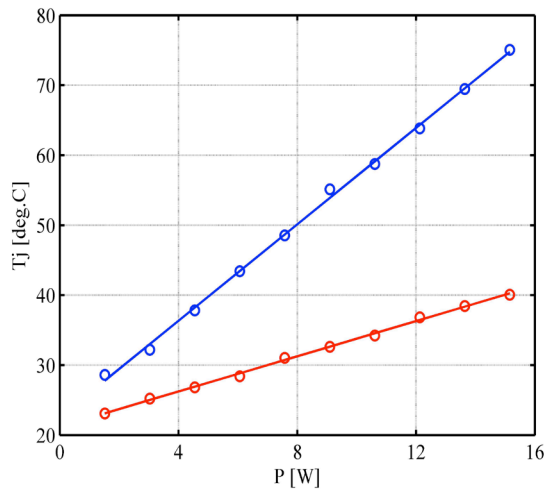


Figure 4. Junction temperature of LED versus electrical power of LED. Case a (blue) and case b (red).

TABLE 1. THE MEASURED THERMAL RESISTANCES.  $R_{p-amb}$  IS THERMAL RESISTANCE BETWEEN PLATE AND AMBIENT,  $R_{p-hs}$  BETWEEN PLATE AND HEATSINK, AND  $R_{hs-amb}$  BETWEEN HEATSINK AND AMBIENT.

	$R_{p-amb}$	$R_{p-hs}$	$R_{hs-amb}$
	[K/W]	[K/W]	[K/W]
Case a	3.81	0.25	3.56
Case b	0.92	0.29	0.62

Fig. 4. shows the tremendous effect the active cooling has for the junction temperature of LED. Table 1 shows the thermal resistances which can be calculated from the measurements.  $R_{p-hs}$  is thermal resistance which includes one aluminium plate and two thermal crease layers

(TIM). Fig. 5 shows how the junction temperature changes versus the electric current of the TEC with four LED power levels. At all power levels, the minimum junction temperature will be reached at electric current between 2 and 2.5 A. In Fig.6, these results are compared with the case where only the heatsink and the fan are used. Fig. 6 shows the benefit the TEC provides. It can be seen that due to the added aluminium plate, the TEC and the additional TIM layer in case c, some cooling effect of TEC is needed to reach the same cooling effect of case b. By using the optimal TEC electric current the junction temperature can be reduced at every power level of the LED. According the manufacturers data, 20 °C reduction in the junction temperature means approximately 5.3% increase in light generation [9].

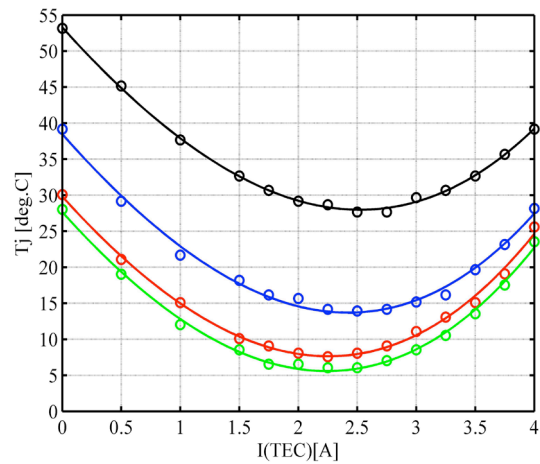


Figure 5. Junction temperature versus electric current of TEC with four power levels of LED. Measurements for case c, where one TEC, heatsink and fan are used.  $P_{LED,electrical}$  is 14.1W (black), 7.05W (blue), 3.53W (red) and 1.76W (green).  $P_{fan,electrical}$  is 0.5W. Ambient temperature is 23 °C.  $R_{j-c}$  is 0.4 °C/W and thermal power of the LED is estimated to be 80% of  $P_{LED,electrical}$ .

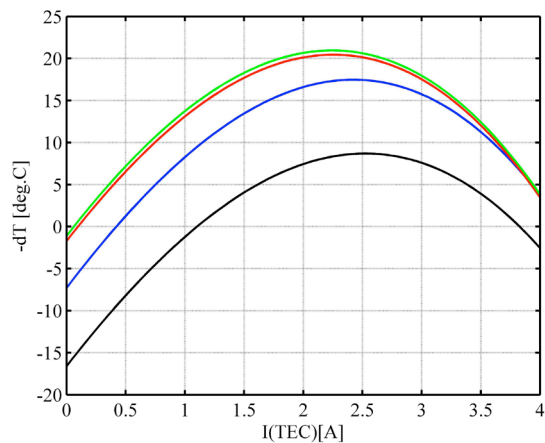


Figure 6. The reduction of junction temperature while using the TEC.  $P_{LED,electrical}$  is 14.1W (black), 7.05W (blue), 3.53W (red) and 1.76W (green). Ambient temperature is 23 °C.  $R_{j-c}$  is 0.4 °C/W and thermal power of the LED is estimated to be 80%  $P_{LED,electrical}$ .

Fig. 7 presents the junction temperature versus the electrical power of TEC. The results have been calculated

by using interpolated values for the electrical resistance of TEC.

The comparison between the measured cases shows that the lowest junction temperature will be with the combination of TEC+heatsink+fan if the electrical current of TEC is 1-4 A. If the current is less than 1 A, the combination heatsink+fan is better in lower LED powers. For example if the electrical current is 0.5 A and the electrical power of LED is less than 7 W. In case only the heatsink is used the junction temperature still remains under 85 °C, the temperature the manufacture has used in the specifications [9].

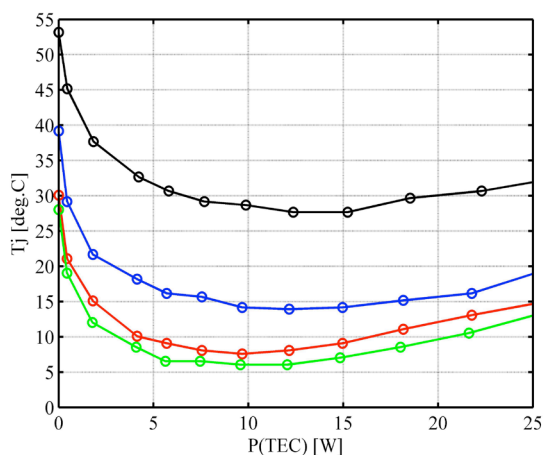


Figure 7. Junction temperature versus the electrical power of TEC.  $P_{LED,electrical}$  is 14.1W (black), 7.05W (blue), 3.53W (red) and 1.76W (green). Ambient temperature is 23 °C.  $R_{j-c}$  is 0.4 °C/W and thermal power of LED is estimated to be 80% of  $P_{LED,electrical}$ .

#### IV. MODELLING WORK

##### A. Modelling using FEM tools

In this study, also FEM simulations were utilized. First a model for the TEC was created. Then some heat transfer simulations were executed to solve the steady-state cases. Supplementary CFD simulations for thermal convection caused by the air flow were executed. Comsol Multiphysics software version 5.0 with the heat transfer and the CFD module was used. Most of the material parameters were found in the software library. However for bismuth telluride electrical conductivity and Seebeck coefficient must be set by the user to match the values of the specific TEC component. Iterative simulations were executed and as a result, the electrical resistance and the maximum temperature difference between cold and hot plates matched the values shown on the component's data sheet.

It was obvious that the simulation case was better to be divided in two parts. The LED module, the TEC and the aluminium plates were simulated using the Heat Transfer module. In this simulation the heatsink and the fan were

modelled by defining the equivalent thermal resistances for the combination (Fig. 8). The operation of the heatsink and the fan is addressed by computational fluid dynamics simulations which uses the CFD module of the software. These simulations requested boundary layer meshing, use of a turbulent flow model and rather long simulation times. This was the reason why the simulation was better to be divided into two parts. Fig. 9 shows air velocity generated by the fan operating at 0.5 W power.

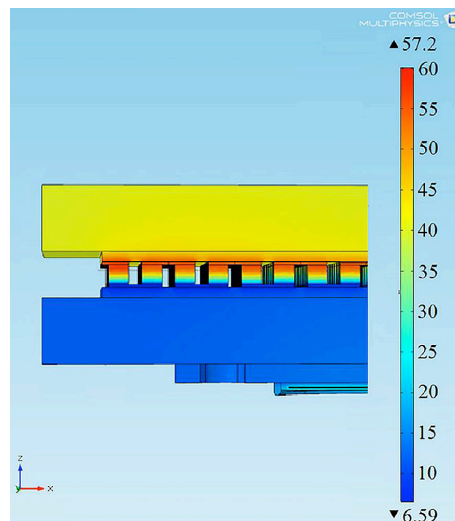


Figure 8. Surface temperature [°C]. One fourth of the LED module and the TEC. FEM-simulation.  $P_{LED,electrical}$  is 14.1 W,  $I_{TEC}$  is 2.5A,  $R_{hs-amb}$  is 0.5 °C/W. Ambient temperature is 23 °C.

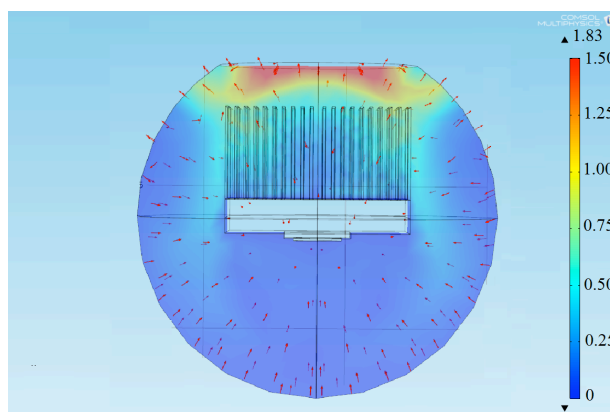


Figure 9. Air velocity [m/s] generated by the fan. The figure shows a vertical slice taken from the middle of the heatsink.  $P_{fan,electrical}$  is 0.5 W.

##### B. Modelling using electric circuit simulator

Equations (1-3) suggest that it is possible to write a rather simple spice model for TEC by creating an electrically equivalent circuit representing the thermal behaviour of TEC and the associated heat dissipation structures. The principles how to form an electrically equivalent circuit for TEC have been presented in several papers [10-15]. The analogy between thermal and electrical parameters is

the following: Thermal flow/heat powers are presented as electric currents, temperatures are voltages, thermal resistances are ohmic resistances and heat capacities are electrical capacitances. Temperatures are presented as Kelvins and the absolute zero temperature is equivalent to electrical ground. The lumped model for an equivalent electrical circuit is often represented in the form as shown in Fig. 10. Alternative forms are represented in papers [12-13]. Forming node equations for  $T_c$  or  $T_h$  results in the same equations (1-2) for  $q_c$  or  $q_h$ .

Seebeck coefficient  $\alpha_m$ , thermal resistance  $\theta_m$  and electrical resistance  $R_m$  are needed for the model. Capacitances in the model are caused by the alumina plates on cold and hot side, added with the capacitance of the bismuth telluride pellets. Half of the capacitance of the pellets is added on the cold side and half to the hot side of TEC. These values may not be available from TEC's data sheets and need to be calculated using material characteristics. Data sheets usually provide values for some parameters like  $V_{max}$ ,  $I_{max}$ ,  $Q_{max}$  and  $\Delta T_{max}$ . These values are usually given at one or two temperatures. Using these values,  $R_m$ ,  $\theta_m$  and  $\alpha_m$  can be calculated. In the model in Fig. 10, these values are interpolated using the values given by the manufacture of TEC at two temperatures, namely for hot side temperatures 25 °C and 50 °C. The developed spice model outputs interpolated values for these parameters.

$$R_m [ \Omega ] = \frac{V_{max} (T_h - \Delta T_{max})}{I_{max} T_h} \quad (6)$$

$$\theta_m [ K/W ] = \frac{\Delta T_{max}}{I_{max} V_{max}} \frac{2T_h}{T_h - \Delta T_{max}} \quad (7)$$

$$\alpha_m [ V/K ] = \frac{V_{max}}{T_h} \quad (8)$$

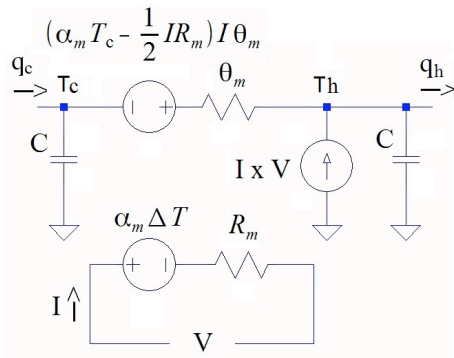


Figure 10. The lumped model of TEC is represented using equivalent electrical components.

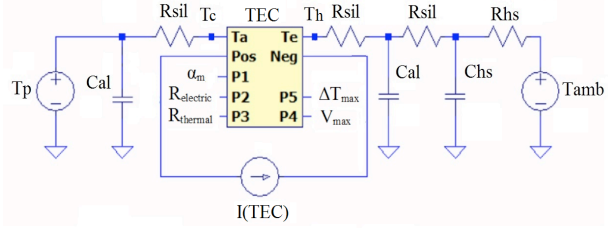


Figure 11. Spice model for TEC. Simulation for case c in Fig 2. The model uses and outputs the linearly interpolated values of  $\alpha_m$ ,  $R_{electric}$ ,  $R_{thermal}$ ,  $V_{max}$  and  $\Delta T_{max}$ .

### C. Capacitances of the spice model

For a steady-state thermal solution capacitances in the model are not required. But for a time dependent simulation they are requested. For the TEC (TEC1-12706, Hebei I.T Co. Ltd. Shanghai) used in the experiment the capacitances will be calculated. Alumina,  $Al_2O_3$ , plates of the TEC have dimensions of 40 mm x 40 mm x 0.8 mm. Aluminium plates have dimensions of 50 mm x 50 mm x 5 mm. The number of bismuth telluride,  $Bi_2Te_3$ , pellets of the TEC is 127. Each pellet has dimensions of approximately 1.5 mm x 1.5 mm x 1.5 mm. Table 2 shows the rest of the material data and the calculated values for the capacitances.

TABLE II. THE THERMAL CAPACITANCES OF THE SPICE MODEL

	Specific heat $J/(m^3 K) \cdot 10^{-6}$	Volume $\cdot 10^{-6}$	Capacitance J/K
Aluminium plate	3.40	12.50	42.50
Alumina plate	3.30	1.28	4.22
Bismuth-tellurium	1.50	0.41	0.64
Heatsink	3.40	47.78	162.44

### D. Resistances of the model

Thermal resistances can be calculated according to the Fourier law of heat conduction.

$$\theta_{thermal} = \frac{s}{Ak} \quad (9)$$

where  $s$  = length of the material parallel to heat flow [m]  
 $A$  = cross sectional area [m<sup>2</sup>]  
 $k$  = thermal conductivity [W/(mK)]

The thermal resistance of the alumina plates, assuming alumina 96% and  $k_{alumina} = 24.7$  W/(mK), will be 0.020 K/W. The relatively small value indicates alumina is a very good thermal conductor. Thermal paste is often a silicone based compound. Its thermal conductivity is normally in range 0.2-0.3 W/(mK), maximum is typically 2 W/mK. Assuming the thickness of the paste layer to be 0.05 - 0.1 mm, thermal conductivity of 0.3 W/(mK), results  $\theta_{paste} = 0.1 - 0.2$  K/W. The thermal resistance of the aluminium plate using  $k_{Al} = 237$  W/(mK) will be

0.008 W/K. The thermal resistance  $\theta_m$  (in Fig 10) can be approximated to be the sum of  $\theta_{\text{alumina}}$ ,  $\theta_{\text{paste}}$  and  $\theta_{\text{aluminium}}$ . The thermal resistance of the paste and the aluminium plate can also be calculated from the measurements of setup a in Fig 2.

TABLE III. THE THERMAL RESISTANCES OF THE SPICE MODEL

	Thermal conductivity, W/(mK)	Area, m <sup>2</sup> 10 <sup>-3</sup>	Length, m 10 <sup>-3</sup>	Thermal resistance, K/W
Aluminum plate	237	2.5	5	0.01
Alumina plate	24.7	1.6	0.8	0.02

### E. Spice model

LTSpice IV has been used to run the model. The simulation is a DC-simulation which executes very fast. It takes only a fraction of a second. The model could be extended to the LED junction by adding the  $R_{j-c}$  resistance in the model. As the experimental work provides the measured temperatures of the aluminium plate on the cold side it is reasonable to set  $T_p$  to present this temperature. Junction temperature can be easily calculated using equation 10.  $R_{j-c}$  is 0.4 K/W for the used LED module. The complete spice model is listed in appendix A.

$$T_j = T_p + R_{j-c} P_{LED} \quad (10)$$

## V. USING THE SPICE MODEL

### A. Steady-state condition simulation

Simulations have been done in steady-state conditions. The results have been compared with the measured values shown in Fig. 5. Table 4 lists results for two power levels of LED. The lumped model for TEC assumes the temperature profiles on cold and hot sides are constants. As far this assumption can be accepted the lumped model results accurate results. In reality there are variations in temperatures along the TEC surfaces. Therefore each bismuth telluride pellet is slightly at different temperature. This causes changes to the material parameters. To improve accuracy, a distributed parameter model can be used. Use of the distributed model requires that the spice model should be integrated in to FEM simulator. Some authors report much improved accuracy while using a distributed model [12]. The idea can be developed backward and consider whether it would be reasonable to use distributed control for the separated elements of TEC. This scheme would lead to the more efficient use of TEC and higher value for COP [16].

Accuracy of the lumped model in steady-state condition was investigated by comparing the measured and simulated temperatures of the heatsink. The model needs a value for  $R_{hs-amb}$ . The value can be taken from table 1 or from the FEM simulations results. The model can be made to match the measured values by optimizing R in the set of equations (11) for getting the minimum  $\sum error^2$ .

qh is calculated by using equation (2).  $R = R_{\text{lim}} + R_{\text{hs-amb}}$ . The number of LED power steps is m and the number of simulated  $I_{TEC}$  steps is n. If the optimization is done over the hole range of  $I_{TEC}$ , R is 0.57 °C/W. Better accuracy in near the optimum value of  $I_{TEC}$  can be reached by discarding the values of low  $I_{TEC}$ . This moves R closer to 0.65 °C/W. By choosing  $R_{hs-amb} = 0.55$  and  $R_{\text{lim}} = 0.1$  results in accuracy < 1 % for  $I_{TEC} < 2$  A, and accuracy < 3 % for  $I_{TEC} < 4$ A.

$$\sum_{i=1}^m [g_h(i) - R \sum_{j=1}^n (T_{amb} - T_{hs}(j, i))]^2 = \sum_{i=1}^m error(i)^2 \quad (11)$$

### B. Time dependent simulation

Time dependent simulation for the spice model executes fast. Fig.12 shows the transient response of the case where both LED and TEC electric currents are switched on at the same moment.  $P_{LED}$  is 14.1 W and the TEC electric current is 2 A. The operation condition is close the maximum cooling effect and close the point of the best match of the model to the measured temperatures. Fig.12 shows both the measured and the simulated temperatures of the heatsink. According to these results, the temperature first increases fast then slower and finally settles within 12 minutes. Fig. 12 shows that the simulated curve settles faster than the curve fitted to the measured values. There are two potential reasons for the difference. Either it is caused by the heat capacity of the fan which couldn't be included in the model, or some other inaccuracy of the simulation model. If the heat capacity on the hot side of TEC would be slightly increased, the simulated results would better fit the measured results. Fig. 13 shows the switch off case. The LED and the TEC are switched off at the same moment, but the fan stays operating. In this case the simulated and the measured values fit much better together. This suggests that the reason for the difference is not the fan. The difference is however rather small, maximum 3 °C in Fig. 12.

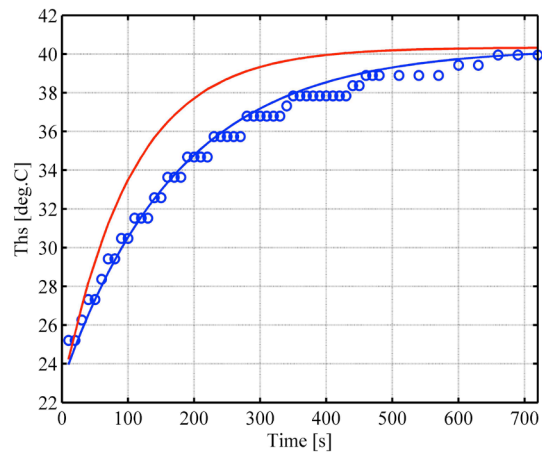
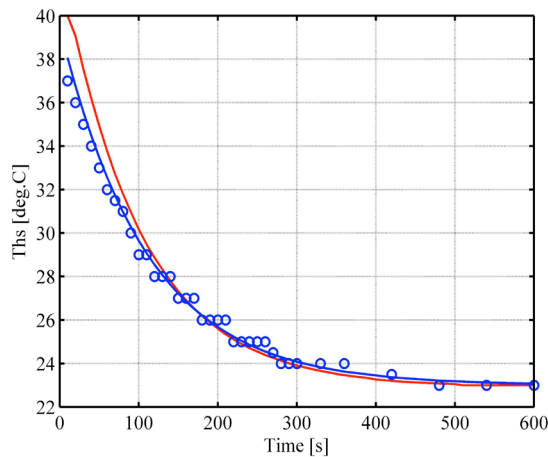


Figure 12. The switch on transient. The measured (blue) and the simulated (red) temperature of the heatsink  $T_{hs}$ .  $P_{LED}$ , electrical is 14.1 W and  $I_{TEC}$  is 2.0 A. In the initial state, the LED module and the TEC are switched off and hole setup is at ambient temperature 23 °C.

Figure 13. The switch off transient. The measured (blue) and the



simulated (red) temperature of the heatsink  $T_{hs}$ . Before switch off, a steady-state condition prevails and PLED, electrical is 14.1 W and ITEC is 2.0 A.

## VI. CONCLUSIONS

An LED-module and its active cooling has been studied. The active cooling uses a thermoelectric module, a heatsink and a fan. The fundamental operation of TEC has been presented. An experimental setup has been constructed and measured. The cooling has been studied also by using simulation tools. FEM simulations have been used to address the heat transfer in the setup. These simulations resulted in the steady-state and the time depending solutions for the temperatures. The behaviour of the fan has been addressed by executing CFD simulations. The CFD simulations resulted in air speed around the heatsink and thermal resistance between the heatsink and ambient. It is also possible to simulate thermal transfer and the operation of TEC by using a lumped model in a standard electrical circuit simulator. Such a model has been developed for the TEC. This model has been composed of standard spice compatible elements. A steady-state thermal solution can be found by executing a simple DC-simulation for the equivalent electrical model. Time dependent thermal solutions have been found by executing transient simulations. The simulated and the measured results match quite well together. The model can be made accurate for limited ranges of TEC current. For a larger range of TEC current the accuracy of the model decreases. Compared with the FEM simulations the lumped model spice simulations provide the average temperatures of the setup much faster and with much less work.

## ACKNOWLEDGMENT

Comsol, Inc. granted a test period license for Multiphysics software ver. 5.0 to be used in this study. I would like to thank the personnel of Comsol office in Helsinki.

## REFERENCES

- [1] M. Kamrul Russel, Dan Ewing, and Chan Y. Ching, "Numerical and Experimental Study of a Hybrid Thermoelectric Cooler Thermal Management System for Electronic Cooling", IEEE

Transaction on components, packaging and manufacturing technology, p. 1608-1616, vol. 2, no. 10, October 2012.

- [2] H. Julian Goldsmid, "Review: Bismuth Telluride and Its Alloys as Materials for Thermoelectric Generation", Open access: [www.mdpi.com/journal/materials](http://www.mdpi.com/journal/materials), ISSN 1996-1944, 2014.
- [3] Je-Hyenong Bahk, Megan Youngs, Kazuaki Yazawa, Ali Shakouri, Oxana Pantchenko, "An online simulator for thermoelectric cooling and power generation", IEEE 2013.
- [4] Junhui Li, Bangke Ma, Ruishan Wang, Lei Han, "Study on a cooling system based on thermoelectric cooler for thermal management of high-power LEDs", Microelectronics Reliability Journal, p. 2210-2215, vol 51, 2011. <http://dx.doi.org/10.1016/j.microrel.2011.05.006>
- [5] Daliang Zhong, Hong Qin, Changhong Wang, Zecheng Xiao, "Thermal Performance of Heatsink and Thermoelectric Cooler Packaging Designs in LED", 11 th. International Conference on Electronic Packaging Technology & High Density Packaging, IEEE, 2010.
- [6] Nan Wang, Chang-hong Wang, Jun-xi Lei, Dong-sheng Zhu, "Numerical Study on Thermal Management of LED Packaging by Using Thermoelectric Cooling", International Conference on Electronic Packaging Technology & High Density Packaging (ICEPT-HDP), IEEE 2009. <http://dx.doi.org/10.1109/icept.2009.5270715>
- [7] Jean Dumitru, Alexandru M. Morega, Diego G. Chamorro and Mihaela Morega, "Numerical Simulation of Thermoelectric Heat Transfer Management", IEEE 2012.
- [8] Yu-Wei Chang, Chih-Chung Chang, Ming-Tsun Ke, Sih-Li-Chen, "Thermoelectric air-cooling module for electronics devices", Applied Thermal Engineering, p. 2731-2737, vol 29, 2009. <http://dx.doi.org/10.1016/j.applthermaleng.2009.01.004>
- [9] Cree Xlamp CXA2011 product family data sheet, CLD-DS40 rev 6. Cree Inc.
- [10] Simon Lineykin, Sam Ben-Yaakov, "PSPICE-Compatible Equivalent Circuit of Thermoelectric Coolers", Power Electronics Specialists Conference, PESC'05, p. 608-612, IEEE 2005. <http://dx.doi.org/10.1109/pesc.2005.1581688>
- [11] Simon Lineykin, Sam Ben-Yaakov, "Analysis of Thermoelectric Coolers by Spice-Compatible Equivalent-Circuit Model", IEEE Power Electronics Letters, p. 63-66, vol. 3, no. 2, June 2005. <http://dx.doi.org/10.1109/LPEL.2005.846822>
- [12] D.Mitrani, J.Salazar, A.Turó, M.J.Carcia, J.A. Chávez "Lumped and Distributed Parameter Spice Models of TE Devices Considering Temperature Dependent Material Properties", EDA Thermic, Budapest, p. 202-207, Hungary, 17-19 September, 2007.
- [13] Daniel Mitrani, José Antonio Tomé, Jordi Salazar, Antoni Turó, Miguel Jesús García, "Methodology for Extracting Thermoelectric Module Parameters", IEEE Transactions on Instrumentation and measurements, p. 1548-1552, vol. 54, no. 4, August 2005. <http://dx.doi.org/10.1109/TIM.2005.851473>
- [14] Mihail Octavian Cernaianu, Aurel Gontean, "High-accuracy thermoelectrical module model for energy-harvesting systems", IET Circuits Devices Syst., p. 114-123, vol. 7, no. 3, 2013. <http://dx.doi.org/10.1049/iet-cds.2012.0227>
- [15] Chakib Alaoui, "Testing and simulation of solid state heating and cooling", International Journal of Engineering Science and Technology, p.1636-1641, vol. 3, no. 2, Feb. 2011.
- [16] R.D. Harvey, D.G. Walker, K.D. Frampton, "Enhancing Performance of Thermoelectric Coolers Through the Application Distributed Control, IEEE Transactions on components and packaging technologies, p. 330-336, vol 30, no 2, June 2007. <http://dx.doi.org/10.1109/TCAPT.2007.898376>

## AUTHOR

**Mika Maaspuro** is with Aalto University, School of Electrical Engineering, P.O. Box 13000, FI-00076 Aalto, Finland (mika.maaspuro@gmail.com)

Submitted 04 May 2015. Published as resubmitted by the author 25 June 2015.

PAPER  
EXPERIMENTING AND SIMULATING THERMOELECTRIC COOLING OF AN LED MODULE

APPENDIX I. TEC SPICE MODEL LIST.

```
.subckt TEC Ta Te Pos Neg AX RX PX VMX DTM
RX Pos 0 1 Meg
E1 Pos 1 VALUE {V(Te,Ta)*V(VMX)/V(Te)}
X1 1 Neg Te 0 Rm_RES
E2 90 0 Pos Neg 1
H1 91 0 E1 1
E3 Ta 2 VALUE {V(Te)*V(91)*(V(VMX)/V(Te))
*(V(DTM)/(V(IMX)*V(VMX)))**2/(1-V(DTM)/V(Te))}
E4 2 3 VALUE {V(91)*V(91)*-0.5*(V(VMX)/V(IMX))
*(1-V(DTM)/V(Te))*(V(DTM)/(V(IMX)*V(VMX)))
*(2/(1-V(DTM)/V(Te)))}
X2 3 Te Te 0 Rt_RES
G1 0 Te VALUE {V(91)*V(90)}
X3 Te DTM dTMax_lin
X4 Te VMX Vmax_lin
X5 Te IMX Imax_lin
E6 AX 0 VALUE {V(VMX)/V(Te)}
E7 RX 0 VALUE {(V(VMX)/V(IMX))*(1-V(DTM)/V(Te))}
E8 PX 0 VALUE {(V(DTM)/(V(IMX)*V(VMX)))
*(2/(1-V(DTM)/V(Te)))}

C1 Ta 0 4.54
C2 Te 0 4.54
.ends TEC
```

APPENDIX II. INTERPOLATING THE VALUES OF R<sub>M</sub>, Φ, V<sub>MAX</sub>, I<sub>MAX</sub>, dT<sub>MAX</sub>. WITH THE GIVEN VALUES THE MODEL IS FOR THE SPECIFIC TEC USED IN THIS STUDY.

```
.subckt Rm_RES 1 2 4 5 Params: Vmax=14.4 Imax=6.4 dTmax=66
ERm 1 3 VALUE {I(Vsense)*(Vmax/Imax)*(1-dTmax/V(4,5))}
Vsense 3 2 DC 0V
.ends Rm_RES

.subckt Rt_RES 1 2 4 5 Params: Vmax=14.4 Imax=6.4 dTmax=66
Ephi 1 3 VALUE {I(Vsense)*(dTmax/(Imax*Vmax))
*(2/(1-dTmax/V(4,5)))}
Vsense 3 2 DC 0V
.ends phi_RES

.subckt dTMax_lin 1 2 Params: Te1=298 Te2=323 dTmax1=66
dTmax2=75
E1 2 0 VALUE {dTmax1+((dTmax2-dTmax1)/
(Te2-Te1))*(V(1)-Te1)}
.ends dTMax_lin

.subckt Vmax_lin 1 2 Params: Te1=298 Te2=323 Vmax1=14.4
Vmax2=16.4
E1 2 0 VALUE {Vmax1+((Vmax2-Vmax1)/(Te2-Te1))*(V(1)-Te1)}
.ends Vmax_lin

subckt Imax_lin 1 2 Params: Te1=298 Te2=323 Imax1=6.4 Imax2=6.4
E1 2 0 VALUE {Imax1+((Imax2-Imax1)/(Te2-Te1))*(V(1)-Te1)}
.ends Imax_lin
```